

Radio Frequency Noise in IFO Sensing and Control System

Nolan King

Mentors: Dick Gustafson and Keita Kawabe

September 28, 2018

Abstract

Radio Frequency (RF) signals are used in the sensing and control subsystem of the interferometer to lock the output port to a dark fringe. This is necessary to maintain the sensitivity of the instrument. RF noise in this subsystem can cause the interferometer to lose lock or cause incorrect readings such as whistles in the differential arm length signal (DARM) as read at the output port. It was previously discovered that a significant contributor to RF noise in the sensing and control system were the ground isolation transforms known as baluns, making a redesign of the component necessary. A corrected design is proposed and prototyped and the resulting attenuation of RF noise is measured.

1 Background

Radio Frequency (RF) oscillators are utilized to generate RF signals for various systems in the IFO. For example, RF sidebands at 9 MHz and 40 MHz are used to generate an error signal for the length of the arm, to be fed back to the mirror position actuator for correction. This RF noise can cause whistles in the response spectrum of the IFO, or generate incorrect feedback in the control system causing the IFO to lose lock. Previous investigation at LHO has found that the transmission lines in the ISC racks exhibit cross talk between these RF signals. Specifically, it was found that the ground isolation transformers, known as baluns, were the primary cause of RF radiation and coupling between lines.

A balun is a class of devices that utilize a transformer to convert a signal from a balanced representation, such as a differential signal transmitted on a twisted pair of conductors, to an unbalanced representation, such as those propagated by coaxial transmission lines. The name "balun" is a portmanteau of "balanced to unbalanced". The particular baluns found on the patch panels of the ISC racks are coaxial to coaxial transformers designed to block any DC offset on the RF signals and DC or 60 Hz noise between separate grounds of the racks. The purpose of the present investigation is to develop repeatable balun modification procedures that provide maximum attenuation of RF noise.

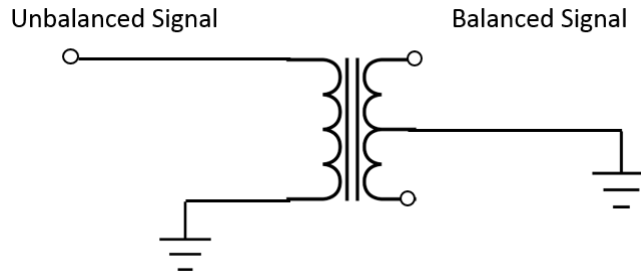


Figure 1: Typical Balun Schematic

2 Investigation

Previous investigation found that nearly all installed baluns were missing the capacitors designed to prevent the balun enclosure from floating with respect to ground. Additionally the wires inside the balun on which the signal is carried were separate stranded wires instead of coaxial wire. This is not optimal for RF because the inconsistent impedance of such a configuration can cause reflections and radiation. Finally, each end of the enclosure was made from circuit board material which does little to shield the circuit from outside radiation or prevent it from radiating.

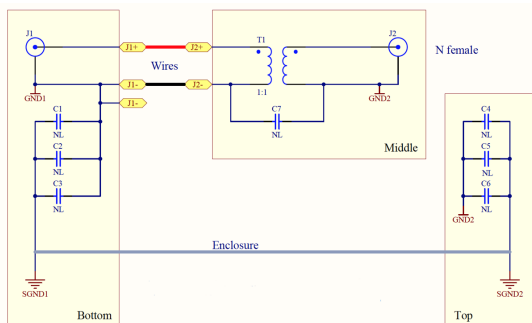


Figure 2: Intended Original Balun Design

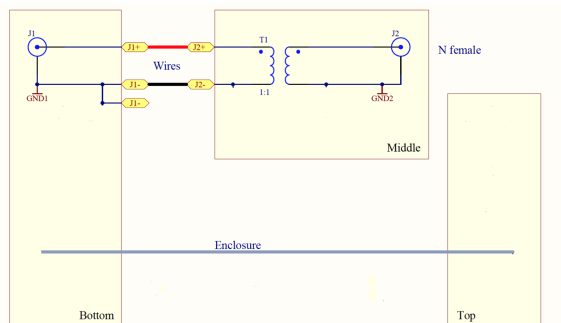


Figure 3: Effective Balun Design

A custom test lead was built to probe the baluns without removing them from the system. The devices used two wrap around leads to measure the potential difference between the two isolated grounds as read at the back shell of the two coaxial connectors of the balun. With a spectrum analyzer and this test lead it was possible to measure the spectrum of the noise radiating into or

out of the line. In principle the back shells of both connectors should be capacitively coupled such that all steady state DC is blocked and any RF signals are shorted to ground. This means any RF signal measured across the back shells of the balun is being radiated into or out of the enclosed line and is not adequately being shorted to ground.



Figure 4: Test lead

A test bench investigation of the devices was conducted using the same measurement device. The balun is connected to the output of a network analyzer, the opposite end is terminated (50Ω), and the test lead is connected to the back shell of both sides of the balun. The response spectrum of the balun was measured and compared to multiple prototypes of replacement balun. See Figure 5.

A copper plate was added to each test balun to ensure the back shell of one connector was connected to body of the balun. The circuit board on the opposite end was fitted with surface mount capacitors to ensure capacitive coupling of the grounds. To verify the efficacy of our measurement technique, measurements of a 9 Mhz line and a neighboring 118 Mhz line were taken before and after replacing the 118 MHz balun with a modified balun. These measurements were compared to and agreed with the spectrum measured on an antenna placed next to the electronics rack.

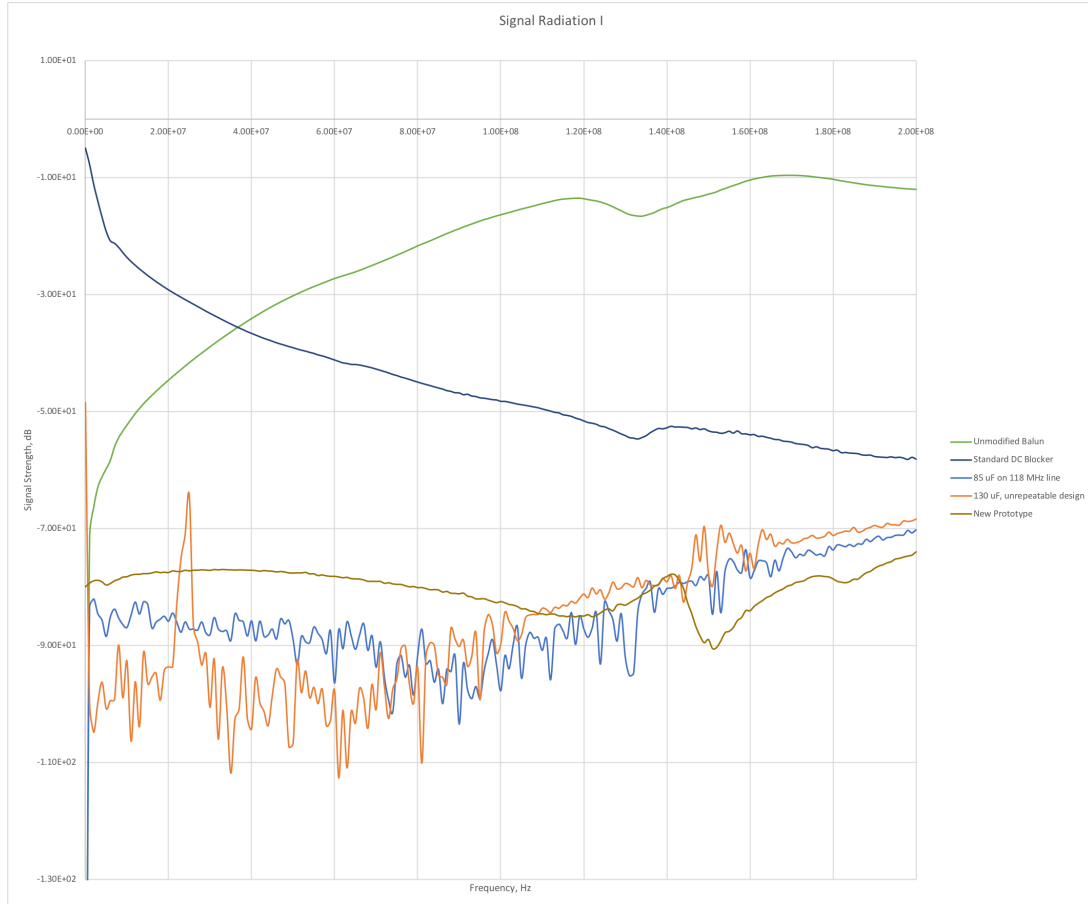


Figure 5: Balun Attenuation, Test Bench

3 Results

Baluns of various capacitance were tested. While some variation was measured as capacitance changed, a greater variation was observed when the configuration of the inner conductor was changed. This suggests the inductance of the wires inside the balun are primarily responsible for radiation. This inductance is determined by the geometry of the conductors (size, shape, and placement).

The greatest noise attenuation was achieved in the 130 μF balun by replacing a stranded conductor ground wire with copper braiding, however attempts to replicate this configuration were unsuccessful. Other attempts at modification included replacing the ground wire with copper tubing, and replacing both wires with coax cabling.

Significant attenuation was achieved in the prototype using a coaxial transmission line. This prototype was revised by replacing the solder cup N type bulkhead connector with a N type to SMA bulkhead adapter, allowing the inside conductor to be replaced with an SMA terminated coax line. This was found to be significantly more repeatable. The unterminated end of the coaxial line was split; the center conductor was connected to the positive end of the transformer, and the shielding to the ground end of the transformer. We found that replacing the balun on the 118 MHz line with a modified balun greatly attenuated the 118 MHz noise on the neighboring 9 MHz line.

A redesign of the printed circuit board inside the balun to better accommodate terminated coaxial transmission lines was drafted and ordered. We placed a surface mount UMCC connector on the transformer circuit board so the coax line may be terminated on both ends, further increasing reproducibility of results.

Three baluns reflecting the final design were fabricated and installed, along with three fabricated using the original copper braid method. Phase and insertion loss measurements were recorded for each of these six baluns before installation in the ISC racks. After installation of these six baluns measurements of the phase through each of the original baluns was recorded and the difference in

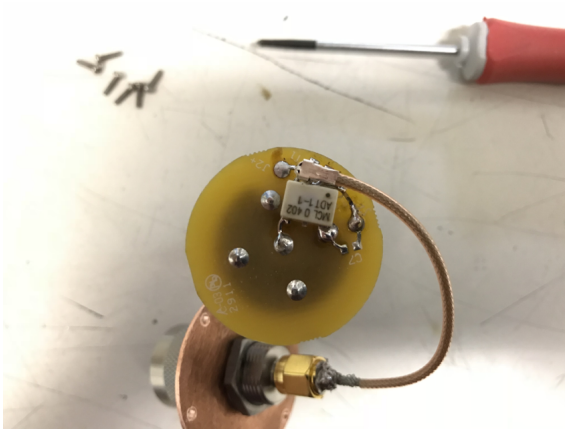


Figure 6: Prototype of Balun Redesign



Figure 7: Prototype of Balun Redesign

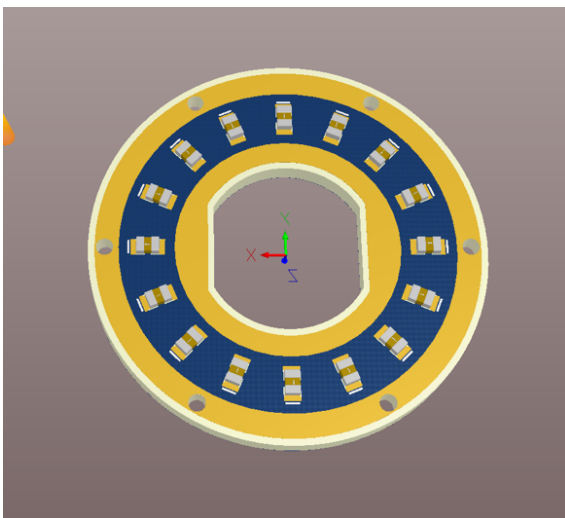


Figure 8: Draft of Balun Redesign

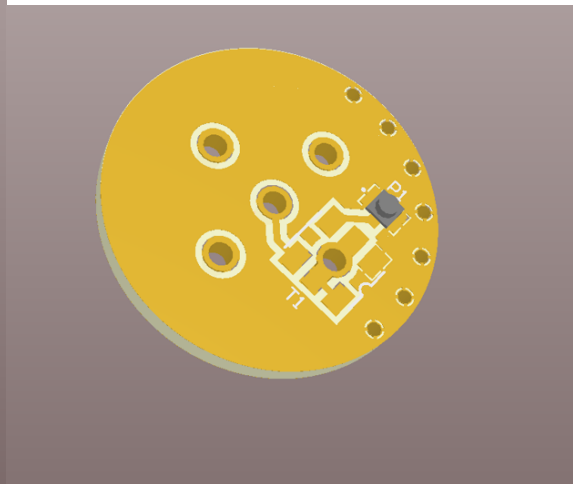


Figure 9: Draft of Balun Redesign

phase at the pertinent frequency of each line was recorded in the Alog for use by the commissioning team.

The installation of these six baluns completed the replacement of a total of eleven baluns that was started during the investigation and testing phase of the experiment. The final noise spectrum of each line was recorded after all baluns had been replaced. Most signals corresponding to leakage and coupling between baluns was attenuated below the noise floor at approximately -65 dBm, while a few remain in the -65 dBm to -55 dBm range. These remaining signals were attenuated by 25 to 30 dB. However, one prominent peak remains on each line's spectrum at approximately 79 MHz. It is thought that this is the 79 MHz signal that is generated for the Acoustic Optic Modulator in the pre-stabilized laser (PSL) rack next to the ISC Rack R1.

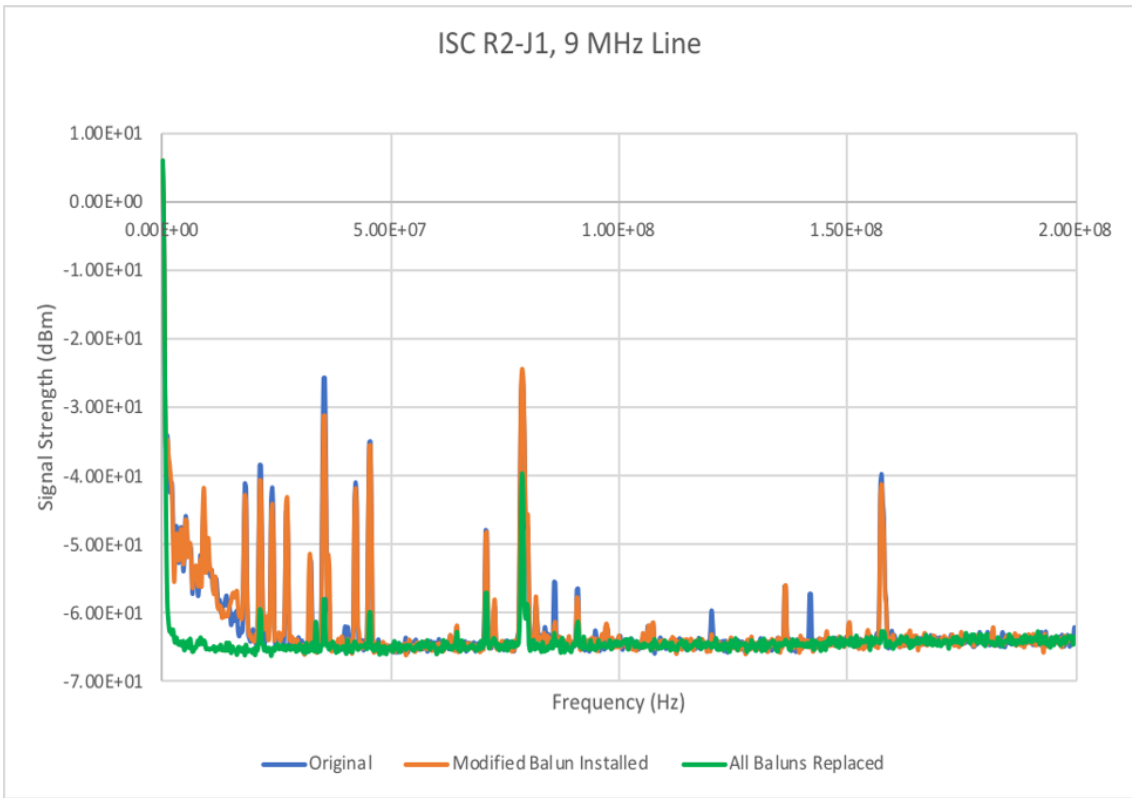


Figure 10: Representative Results of Balun Replacement

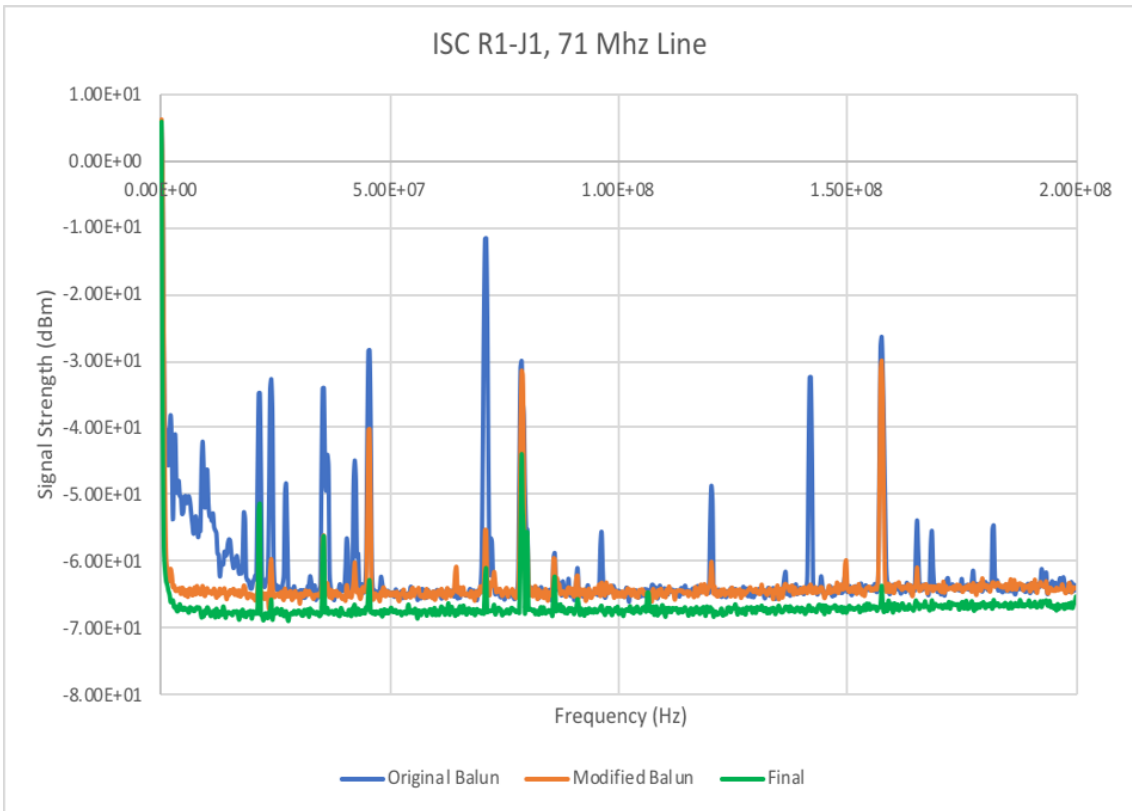


Figure 11: Representative Results of Balun Replacement

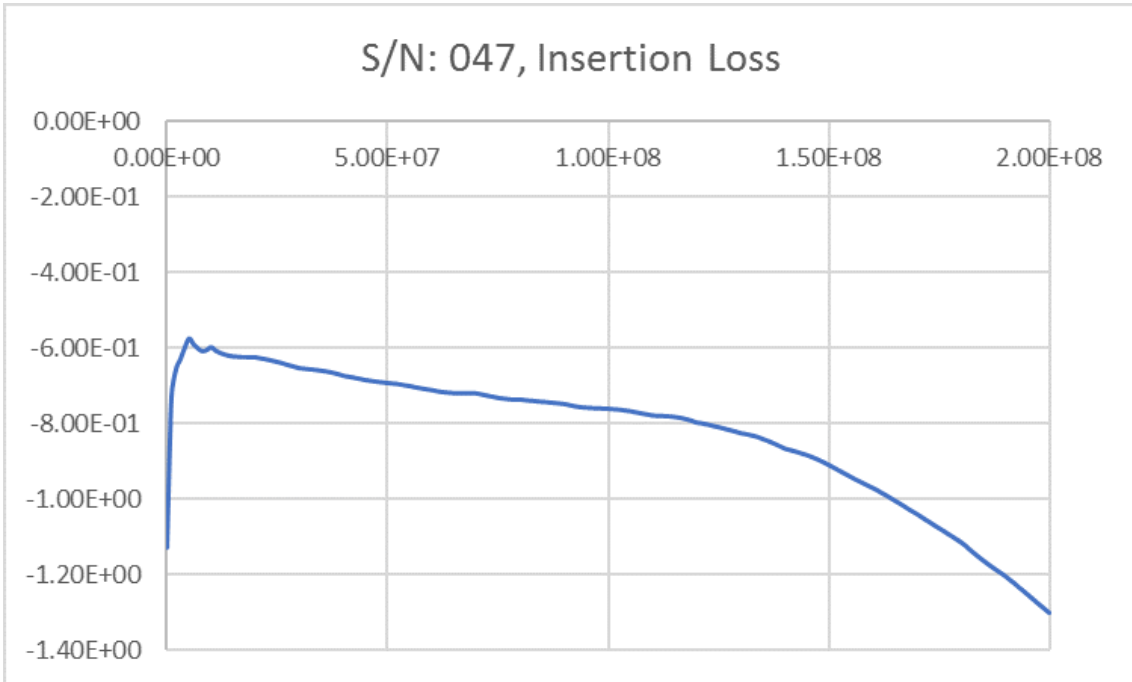


Figure 12: Representative Insertion Loss of New Baluns

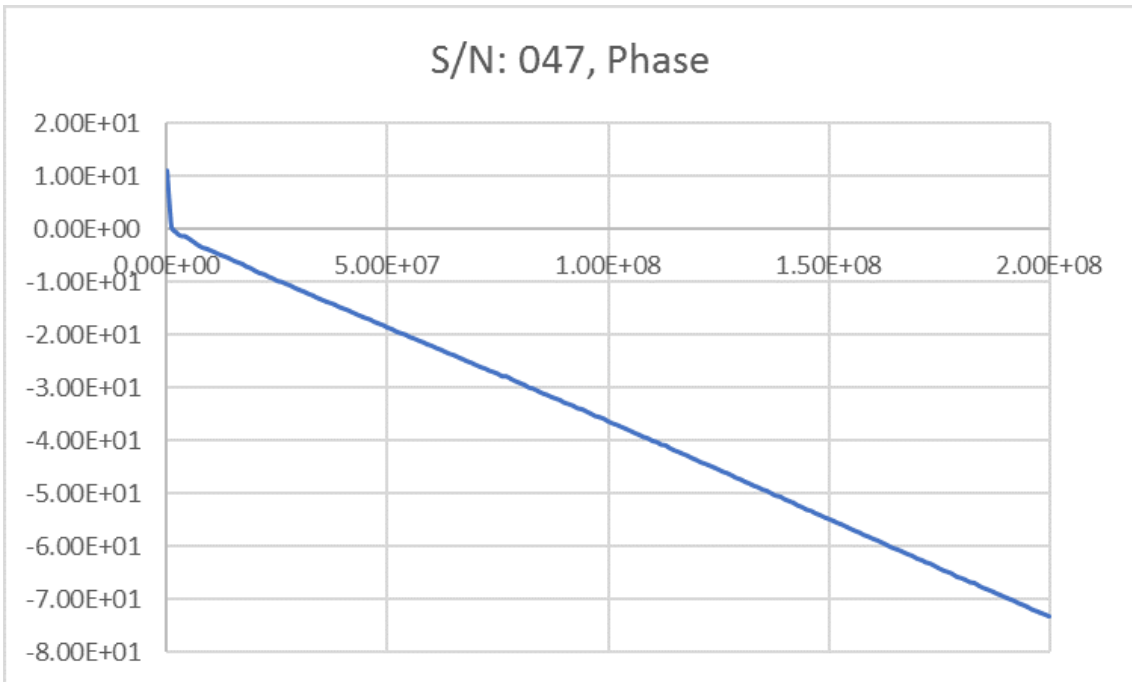


Figure 13: Representative Phase Shift of New Baluns